Malaysian Journal of Mathematical Sciences 7(1): 59-78 (2013)

Mutiple Curved Crack Problems in Antiplane Elasticity for Circular Region with Traction Free Boundary

[1]Noraini Dahalan, [1,2]Nik Mohd Asri Nik Long and [1,2]Zainiddin K. Eshkuvatov

[1]Institute for Mathematical Research, Universiti Putra Malaysia, 43400 UPM Serdang, Selangor,Malaysia

[2]Department of Mathematics, Faculty of Science, Universiti Putra Malaysia, 43400 UPM Serdang, Selangor,Malaysia

E-mail: norainidahalan@yahoo.com

ABSTRACT

The multiple curved cracks in a circular region problem in antiplane elasticity is formulated in terms of hypersingular integral equation in conjunction with the complex variable function method. The obtained hypersingular integral equations are solved numerically using the curve length coordinate method, where the curved crack configurations are mapped on the real axes s with intervals $(-a_i, a_i) = 1, 2, \ldots, n.$. Suitable scheme is used for the determination of the unknown functions. For numerical purposes only a particular case of doubly circular arc cracks is considered, and it is found that the stress intensity factors (SIFs) are higher as the cracks become closer to the circular boundary.

Keywords: antiplane elasticity, hypersingular integral equation, crack opening displacement, stress intensity factors.

1. INTRODUCTION

The crack problems in plane elasticity have been studied extensively by many researchers using various approaches. The stress intensity factor (SIF) is the main interests as the data are imperative predicting the stability of cracked components. The pertubation method is used for solving the various set of slightly curved and kinked cracks problems in plane elasticity by Cotterell *et al.* (1980), Martin (2000) and Chen (1999). Single and multiple cracks problems, formulated in terms of singular and hypersingular integral equations, are found in Chen (2003), Ang (2001), Chen *et al.* (1995), Gray *et al.* (1990), Yan *et al.* (2010), Chen *et al.* (1992) and Nik Long *et al.* (2009), and the interaction between the curved crack and a circular inclusion is studied in Cheesman *et al.* (2000), Chao (1996), Dong (2005) and Hasebe *et al.* (1984). On the other hand, many authors dealt with the problem of cracks inside and outside a circular region by formulating into singular integral equations ((Lin *et al.* (1989), Hong-shan *et al.* (1989)), hypersingular integral equation (Jian *et al.* (2004) and Chen *et al.* (2005)) and for the antiplane problems (Chen *et al.* (2004), Chen *et al.* (1986), Chen (1993), Shen *et al.* (1998) and Zhong-xian (2006)).

In this paper, the system of hypersingular integral equations for multiple curved cracks in antiplane elasticity for a circular region with traction free is formulated, and solved numerically using curved length technique. Some numerical examples are given to demonstrate the behaviour of SIF for different cracks positions inside and outside of a circular boundary.

2. FUNDAMENTAL FORMULAE AND PROBLEM FORMULATION

In antiplane elasticity, the displacement w is everywhere perpendicular to the xy plane. Thus, the displacements are assumed to be in the form of $u=0, v=0, w=w(x,y)$. Hence, the non-vanishing stresses components σ_{zx} and σ_{zy} can be expressed by

$$\sigma_{zx}=G\frac{\partial w}{\partial x},\ \sigma_{zy}=G\frac{\partial w}{\partial y},$$

where G is shear modulus of elasticity.

It is not difficult to show that the displacement component $w(x,y)$ is a harmonic function. Let the complex potential $\phi(z)$ takes the form

$$\phi(z)=Gw(x,y)+if(x,y) \tag{1}$$

where $f(x,y)$ is an analytic function. It is obvious from (1) that

$$Gw(x,y)=\frac{1}{2}\left(\phi(z)+\overline{\phi(z)}\right)$$

and

$$f(x,y)=\frac{1}{2i}\left(\phi(z)-\overline{\phi(z)}\right).$$

From the Cauchy-Riemann condition, the stress components can be written as

$$\sigma_{zx}=G\frac{\partial w}{\partial x}=\frac{\partial f}{\partial y},\ \sigma_{zy}=G\frac{\partial w}{\partial y}=-\frac{\partial f}{\partial x}. \tag{2}$$

From Equations (1) and (2), it is easy to see that

$$\Phi(z)=\phi^{'}\left(z\right)=\sigma_{zx}-i\sigma_{zy}=\frac{\partial f}{\partial y}+i\frac{\partial f}{\partial x}, \tag{3}$$

which gives

$$f(x,y)=\int_{z_0}^{z}\left(\sigma_{zx}dy-\sigma_{zy}dx\right). \tag{4}$$

In Equation (4), the domain of integration is a path connecting the fixed point $z_0=x_0+iy_0$ and the generic point $z=x+iy$ (Muskhelishvilli *et al.* (1958)).

By placing a continuous distribution of doublet dislocation along the curve L, the appropriate complex potential $\phi_p(z)$ takes the form (Chen (2004))

$$\phi_p(z)=\frac{1}{\pi i}\int_L\frac{g(t)dt}{t-z}. \tag{5}$$

Letting the point z approaches t_0^+ and t_0^-, which are located on the upper and lower side of crack faces, the following result is obtained

$$\phi_p^+(t_0)-\phi_p^-(t_0)=2g(t_0)\ \text{or}$$
$$G(w^+(t_0)-w^-(t_0))=2g(t_0).$$

The function $g(t)$ represents the crack opening displacement (COD) function at the crack tips.

For a curved crack in a circular region with the traction free condition on the circular boundary C_R, the appropriate complex potential is

$$\phi(z) = \phi_p(z) + \phi_h(z) \tag{6}$$

where $\phi(z)$ and $\phi_p(z)$ represent the modified and original complex potentials, respectively.

Since the circular boundary is traction free, we have $\mathrm{Im}(z) = 0, z \in C_R$ and from (6), gives

$$\phi_p(z) + \phi_h(z) - \left(\overline{\phi_p(z)} + \overline{\phi_h(z)}\right) = 0, \qquad z \in C_R \tag{7}$$

which leads to

$$\phi_h(z) = \overline{\phi_p}\left(\frac{R^2}{z}\right) = \frac{1}{\pi i}\int \frac{zg(t)d\bar{t}}{R^2 - \bar{t}z}. \tag{8}$$

A derivative of the complex potential $\phi(z) = Gw + if$ in a specified direction of the point z is

$$\frac{\partial(Gw + if)}{\partial n} = \frac{1}{\pi}\int_L \frac{\exp(i\alpha)g(t)dt}{(t-z)^2} + \frac{1}{\pi}\int_L \frac{\exp(i\alpha)R^2 g(t)d\bar{t}}{(R^2 - \bar{t}z)^2}, \tag{9}$$

where α denotes an inclined angle for dz with respect to the x-axis.

From Equation (9), for a point z on the segment $\overline{zz + dz}$, we obtain the following stress components σ_{zn}

$$\sigma_{zn} = G\frac{\partial w}{\partial n} = \frac{1}{\pi}\mathrm{Re}\int_L \frac{\exp(i\alpha)g(t)}{(t-z)^2} + \frac{1}{\pi}\mathrm{Re}\int_L \frac{\exp(i\alpha)R^2 g(t)d\bar{t}}{\left(R^2 - \bar{t}z\right)^2}. \tag{10}$$

For a single curved crack in a circular region with traction free circular boundary, by letting $z \to t_0$ and $\alpha \to \alpha_0$ in (11), a hypersingular integral equation for a curved crack problem in circular region is obtained as follows (Chen (2003))

$$\frac{1}{\pi} f.p \operatorname{Re} \int_L \frac{\exp(i\alpha_0) g(t) dt}{(t-t_0)^2} + \frac{1}{\pi} \operatorname{Re} \int_L \frac{\exp(i\alpha_0) R^2 g(t) d\bar{t}}{(R^2 - \bar{t}t_0)^2} = \overline{P}(t_0),\ t_0 \in L. \quad (11)$$

where α_0 is the angle at the point t_0 on the curve configuration and R is a radius of a circular region. In Equation (11), $\overline{P}(t_0)$ denotes the loading on the crack faces, which is given beforehand.

Consider two curved cracks in a circular region with traction free along the outer circular boundary, and some loading $\sigma_{zn}\left(=G\dfrac{\partial w}{\partial n}\right)$ is applied on the crack faces (Figure 1). The boundary conditions along two crack faces are

$$\sigma_{zn}(t_{j0}) = \overline{P}_j(t_{j0}), \quad (t_{j0} \in L_j, j = 1,2). \quad (12)$$

where $\overline{P}_j\left(t_{j_0}\right)$ $\left(t_{j_0} \in L_j, j=1,2\right)$ are the loading applied on the crack faces.The formulation of the hypersingular integral equation for crack-1 is introduced below. If the COD is placed at point $z = t_1, dz = dt_1,$ and $g_1(t_1)$ is the COD for crack-1, after using Equation (11) and making integration, the traction influence at the point t_{10} denoted by $p_{11}(t_{10})$ can be expressed as follows

$$\frac{1}{\pi} f.p \operatorname{Re} \int_{L1} \frac{\exp(i\alpha_{10}) g_1(t_1) dt_1}{(t_1 - t_{10})^2} + \frac{1}{\pi} \operatorname{Re} \int_L \frac{\exp(i\alpha_{10}) R^2 g_1(t_1) d\overline{t_1}}{(R^2 - \overline{t_1} t_{10})^2}$$
$$= p_{11}(t_{10}),\ t_{10} \in L \quad (13)$$

In addition, from Equation (10), the traction influence at the point t_{10} from COD function $g_2\left(t_2\right)$ for crack-2 is

$$\frac{1}{\pi}\mathrm{Re}\int_{L2}\frac{\exp(i\alpha_{10})g_2(t_2)dt_2}{(t_2-t_{10})^2}+\frac{1}{\pi}\mathrm{Re}\int_{L2}\frac{\exp(i\alpha_{10})R^2 g_2(t_2)d\overline{t_2}}{(R^2-\overline{t_2}t_{10})^2}$$

$$= p_{12}(t_{10}),\ t_{10}\in L. \tag{14}$$

By superposition of the COD for the curved crack-1, $g_1(t_1)$ and the COD for the curved crack-2, $g_2(t_2)$, we obtain the hypersingular integral equation for crack-1 which is

$$\begin{aligned}&\frac{1}{\pi}\mathrm{Re}\, f.p.\int_{L1}\frac{\exp(i\alpha_{10})g_1(t_1)dt_1}{(t_1-t_{10})^2}-\frac{1}{\pi}\mathrm{Re}\int_{L1}\frac{\exp(i\alpha_{10})R^2 g_1(t_1)d\overline{t_1}}{(R^2-\overline{t_1}t_{10})^2}\\&+\frac{1}{\pi}\mathrm{Re}\int_{L2}\frac{\exp(i\alpha_{10})g_2(t_2)dt_2}{(t_2-t_{10})^2}-\frac{1}{\pi}\mathrm{Re}\int_{L2}\frac{\exp(i\alpha_{10})R^2 g_2(t_2)d\overline{t_2}}{(R^2-\overline{t_2}t_{10})^2}\\&=\overline{P_1}(t_{10}),\ t_{10}\in L_1\end{aligned} \tag{15}$$

where $\overline{P_1}\left(t_{10}\right)$ is the given boundary traction shown in Equation (12).

Similarly, the hypersingular integral equation for crack is

$$\begin{aligned}&\frac{1}{\pi}\mathrm{Re}\, f.p.\int_{L2}\frac{\exp(i\alpha_{20})g_2(t_2)dt_2}{(t_2-t_{20})^2}+\frac{1}{\pi}\mathrm{Re}\int_{L2}\frac{\exp(i\alpha_{20})R^2 g_2(t_2)d\overline{t_2}}{(R^2-\overline{t_2}t_{20})^2}\\&+\frac{1}{\pi}\mathrm{Re}\int_{L1}\frac{\exp(i\alpha_{20})g_1(t_1)dt_1}{(t_1-t_{20})^2}+\frac{1}{\pi}\mathrm{Re}\int_{L1}\frac{\exp(i\alpha_{20})R^2 g_1(t_1)d\overline{t_1}}{(R^2-\overline{t_1}t_{20})^2}\\&=\overline{P_2}(t_{20}),t_{20}\in L_2.\end{aligned} \tag{16}$$

In the present study, constant loadings are applied on the faces of two cracks, which take the following form

$$\overline{P_{j_0}}=-p_0,\ \left(t_{j_0}\in L_j, j=1,2\right). \tag{17}$$

Clearly, the formulation can be extended to the case of N (N > 2) curved cracks with traction free condition along circular boundary.

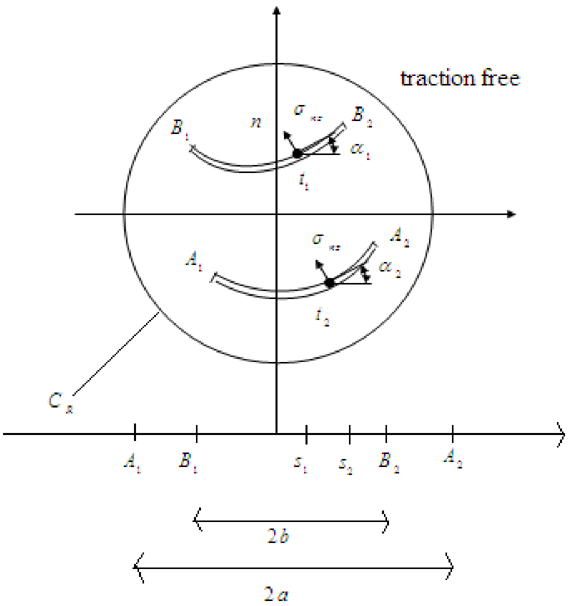

Figure 1: Curve cracks in circular region

3. SOLUTION APPROACH

For the numerical computation of the hypersingular integral equation, the curve length method is suggested (Chen (2003)). For the solution approaches, we consider a particular case of doubly circular arc cracks (Figure 1). The curved configurations are mapped on the real axis s with an interval of length $2a$ and $2b$ respectively. The mapping relation is expressed by the functions $t_1(s_1)$ and $t_2(s_2)$ as follows

$$g_1(t_1)|_{t_1=t_1(s_1)} = \sqrt{a^2 - s_1^2}\,H_1(s_1) \text{ where } H_1(s_1) = H_{11}(s_1) + iH_{12}(s_1) \tag{18}$$

and

$$g_2(t_2)|_{t_2=t_2(s_2)} = \sqrt{b^2 - s_2^2}\,H_2(s_2) \text{ where } H_2(s_2) = H_{21}(s_2) + iH_{22}(s_2). \tag{19}$$

In Equations (18) and (19), $g_1(t_1)$ and $g_2(t_2)$ are chosen in such way that they must satisfy the behaviour of the COD at the vicinity of crack tips. The following substitutions are used:

$$p(t)|_{t=t(s)} = P(s), \; dt = \exp\left(i\alpha\right)ds, \; d\bar{t} = \exp(-i\alpha)ds. \tag{20}$$

Using (18), (19) and (20), Equations (15) and (16) can be written as

$$I_1(s_{10}) + I_2(s_{10}) + I_3(s_{10}) + I_4(s_{10}) = P_1(s_{10}) \tag{21}$$

and

$$L_1(s_{20}) + L_2(s_{20}) + L_3(s_{20}) + L_4(s_{20}) = P_2(s_{20}) \tag{22}$$

where

$$\begin{aligned}
I_1(s_{10}) &= \frac{1}{\pi} f.p.\int_{-a}^{a} \sqrt{a^2 - s_1^2}\, H_1(s_1) \frac{D_1(s_1, s_{10})ds_1}{(s_1 - s_{10})^2};\\
I_2(s_{10}) &= \frac{1}{\pi} \int_{-a}^{a} \sqrt{a^2 - s_1^2}\, H_1(s_1) D_2(s_1, s_{10})ds_1;\\
I_3(s_{10}) &= \frac{1}{\pi} \int_{-a}^{a} \sqrt{b^2 - s_2^2}\, H_2(s_2) \frac{D_3(s_2, s_{10})ds_2}{(s_2 - s_{10})^2};\\
I_4(s_{10}) &= \frac{1}{\pi} \int_{-a}^{a} \sqrt{b^2 - s_2^2}\, H_2(s_2) D_4(s_2, s_{10})ds_2;
\end{aligned}$$

and

$$\begin{aligned}
L_1(s_{20}) &= \frac{1}{\pi} f.p.\int_{-b}^{b} \sqrt{b^2 - s_2^2}\, H_2(s_2) \frac{E_1(s_2, s_{20})ds_2}{(s_2 - s_{20})^2};\\
L_2(s_{20}) &= \frac{1}{\pi} \int_{-b}^{b} \sqrt{b^2 - s_2^2}\, H_2(s_2) E_2(s_2, s_{20})ds_2;\\
L_3(s_{20}) &= \frac{1}{\pi} \int_{-b}^{b} \sqrt{a^2 - s_1^2}\, H_1(s_1) \frac{E_3(s_1, s_{20})ds_1}{(s_1 - s_{20})^2};\\
L_4(s_{20}) &= \frac{1}{\pi} \int_{-b}^{b} \sqrt{a^2 - s_1^2}\, H_1(s_1) E_4(s_1, s_{20})ds_1;
\end{aligned}$$

D_1, D_2, D_3, D_4 and E_1, E_2, E_3, E_4 are respectively given by

$$D_1(s_1, s_{10}) = \operatorname{Re}\left(\frac{\exp(i(\alpha_1 + \alpha_{10}))(s_1 - s_{10})^2}{(t_1 - t_{10})^2} \right);$$

$$D_2(s_1, s_{10}) = R^2 \operatorname{Re}\left(\frac{\exp(i(\alpha_{10} - \alpha_1))}{(R^2 - \overline{t_1} t_{10})^2} \right);$$

$$D_3(s_2, s_{10}) = \operatorname{Re}\left(\frac{\exp(i(\alpha_2 + \alpha_{10}))(s_2 - s_{10})^2}{(t_2 - t_{10})^2} \right);$$

$$D_4(s_2, s_{10}) = R^2 \operatorname{Re}\left(\frac{\exp(i(\alpha_{10} - \alpha_2))}{(R^2 - \overline{t_2} t_{10})^2} \right);$$

$$E_1(s_2, s_{20}) = \operatorname{Re}\left(\frac{\exp(i(\alpha_2 + \alpha_{20}))(s_2 - s_{20})^2}{(t_2 - t_{20})^2} \right);$$

$$E_2(s_2, s_{20}) = R^2 \operatorname{Re}\left(\frac{\exp(i(\alpha_{20} - \alpha_2))}{(R^2 - \overline{t_2} t_{20})^2} \right);$$

$$E_3(s_1, s_{20}) = \operatorname{Re}\left(\frac{\exp(i(\alpha_1 + \alpha_{20}))(s_1 - s_{20})^2}{(t_1 - t_{20})^2} \right);$$

$$E_4(s_1, s_{20}) = R^2 \operatorname{Re}\left(\frac{\exp(i(\alpha_{20} - \alpha_1))}{(R^2 - \overline{t_1} t_{20})^2} \right).$$

Equations (21) and (22) are to be solved numerically. For the numerical computation, the following integration rules developed by Mayrofer and Fisher (1992) are used, which are

$$\frac{1}{\pi} f.p.\int_{-a}^{a} \frac{\sqrt{a^2 - s^2}\, G(s)ds}{(s - s_0)} = \sum_{j=1}^{M+1} W_j(s_0) G(s_j) \qquad (|s_0| < a) \tag{23}$$

and

$$\frac{1}{\pi} \int_{-a}^{a} \sqrt{a^2 - s^2}\, G(s)ds = \frac{1}{M+2} \sum_{j=1}^{M+1} (a^2 - s_j^2) G(s_j), \tag{24}$$

where $G(s)$ is a given regular function, $M \in Z$,

$$s_j = s_{oj} = a\cos\left(\frac{j\pi}{M+2}\right), \quad j = 1,2,3,...,M+1$$

and

$$W_j(s_0) = -\frac{2}{M+2}\sum_{n=0}^{M}(n+1)\sin\left(\frac{j\pi}{M+2}\right)\sin\left(\frac{(n+1)j\pi}{M+2}\right)U_n\left(\frac{s_0}{a}\right).$$

Here $U_n(t)$ is a Chebyshev polynomial of the second kind, defined by

$$U_n(t) = \frac{\sin((n+1)\theta)}{\sin\theta}, \ t = \cos\theta.$$

Denote

$$V_j^n = \sin\left(\frac{j\pi}{M+2}\right)\sin\left(\frac{(n+1)j\pi}{M+2}\right),$$

$H_1(s)$ and $H_2(s)$ are evaluated using

$$H_1(s) = \sum_{n=0}^{M} c_{1n}u_n\left(\frac{s}{a}\right), \ |s| \le a$$

and

$$H_2(s) = \sum_{n=0}^{M} c_{2n}u_n\left(\frac{s}{b}\right), \ |s| \le b$$

where

$$c_{1n} = \frac{2}{M+2}\sum_{j=1}^{M+1} V_j^n H_1(s_1),$$

$$c_{2n} = \frac{2}{M+2}\sum_{j=1}^{M+1} V_j^n H_2(s_2).$$

and $H_1(s_1)$ and $H_2(s_2)$ are define in (18) and (19) respectively.

4. NUMERICAL EXAMPLES

4.1 Example 1

In this example, two half circular arc cracks in circular region is considered Figure 2(a). The calculated results for SIFs at the crack tips of inner and outer crack are expressed as

$$K_{3,A1} = K_{3,A2} = F_{3,A1}(k_1)\sqrt{\pi b_2} \tag{25}$$

$$K_{3,A1} = K_{3,A2} = F_{3,A1}(k_1)\sqrt{\pi b_2} \tag{26}$$

where $b_1 = r_1 \sin\theta$ and $b_2 = r_2 \sin\theta$

For comparison purposes, we use Fredholm integral equation (FIE) of theas in Chen (1993), subjected to the remote stress $\sigma_{nz} = -p_0$. The numerical results are tabulated in Table 1, as well as in Figure (3), with $k_1 = k_2 = 0\cdot 5$ where $k_1 = r_1 / r_2$ and $k_2 = r_2 / R$.

Figures 4 and 5 show the effect of distance between two cracks and a circular Boundary C_R. It is found that for different values of k_1. SIFs for crack-1 (Figure 4(a)) is higher than those of crack-2 (Figure 4(b)). Similar behaviour is observed for different values of k_2 (Figure 5). It is also observed that the SIF increases as the distance between two cracks (with $k_2 = 0\cdot 5$) (Figure 4) and the distance between crack and boundary with (with $k_2 = 0\cdot 5$) (Figure 5) decrease (k_2 and k_1 increase).

4.2 Example 2

Consider two circular arc cracks placed eccentrically inside the circular region (Figure (2b)). The boundary traction is assumed to be $\sigma_{nz} = -p_0$ and the calculated results for SIFs at the crack tips A_1, A_2, B_1 and B_2 are respectively, expressed as

$$K_{3,A_1} = F_{3.A_1}(d_1 / r_1)\sigma_{zn}\sqrt{\pi r_1} \tag{27}$$

$$K_{3,A_2} = F_{3.A_2}(d_1 / r_1)\sigma_{zn}\sqrt{\pi r_1}$$

and

$$K_{3,B_1} = F_{3.B_1}(d_2 / r_2)\sigma_{zn}\sqrt{\pi r_2} \tag{28}$$

$$K_{3,B_2} = F_{3.B_2}(d_2 / r_2)\sigma_{zn}\sqrt{\pi r_2}$$

The calculated values are shown in Figure 6. Observably, as the values of d_1 / r_1 and d_2 / r_2 increase, the SIF increases (Figures 6(a) and (b), respectively). At $\theta = \pi / 2$, the values of the stress intensity factor for F_{B_1} are greater than F_{B_2} decrease, with $d_1 / r_1 = 0 \cdot 5$ (Figure 6(c)).

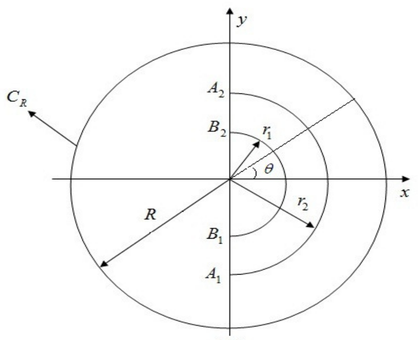

Figure 2(a): Two half circular are cracks in a circular region

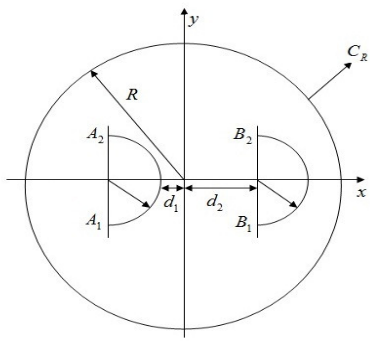

Figure 2(b): Eccentrically half circular are cracks in a circular region

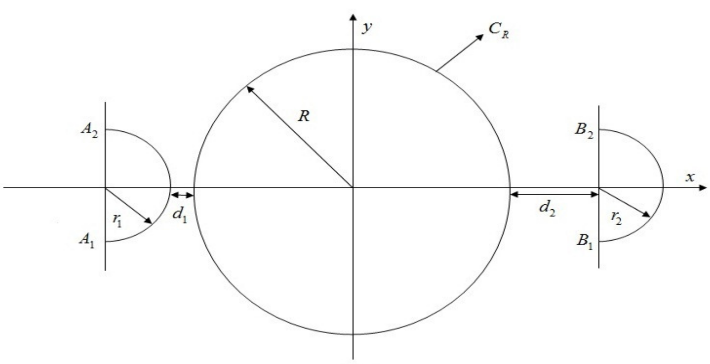

Figure 2(c): Eccentrically half circular are cracks outside a circular hole

4.3 Example 3

Consider two half circular arc cracks placed eccentrically outside the circular region (Figure 2(c)) and the calculated results are shown in Figure (7). The stress is subjected to $\sigma_{nz} = -p_0$ and the SIFs at the crack tips are defined as Equations (27) and (28). The SIF at the cracks tips decrease as the value of d_1 / r_1 increases, with $d_2 / r_2 = 0 \cdot 5$ (Figure 7(a)). Similar behaviour can be seen as d_{12} / r_2, with $d_1 / r_1 = 0.5$ (Figure 7(b)).

TABLE 1: SIFs for $k_1 = 0.5$ and $k_2 = 0.5$

	$F_{A_1} = F_{A_2}$		$F_{B_1} = F_{B_2}$	
σ	**In this paper**	**Chen *et al.* (2004)**	**In this paper**	**Chen *et al.* (2004)**
0	-0.6068	-0.6062	0.4125	0.4105
10	-0.4080	-0.4075	0.6064	0.6045
20	-0.1968	-0.1962	0.8122	0.8118
30	0.0203	0.0201	1.0238	1.0236
40	0.2369	0.2362	1.2346	1.2341
50	0.4463	0.4459	1.4383	1.4379
60	0.6421	0.6401	1.6287	1.6274
70	0.8184	0.8182	1.8002	1.7991
80	0.9698	0.9695	1.9469	1.9464
90	1.0918	1.902	2.0651	2.0646

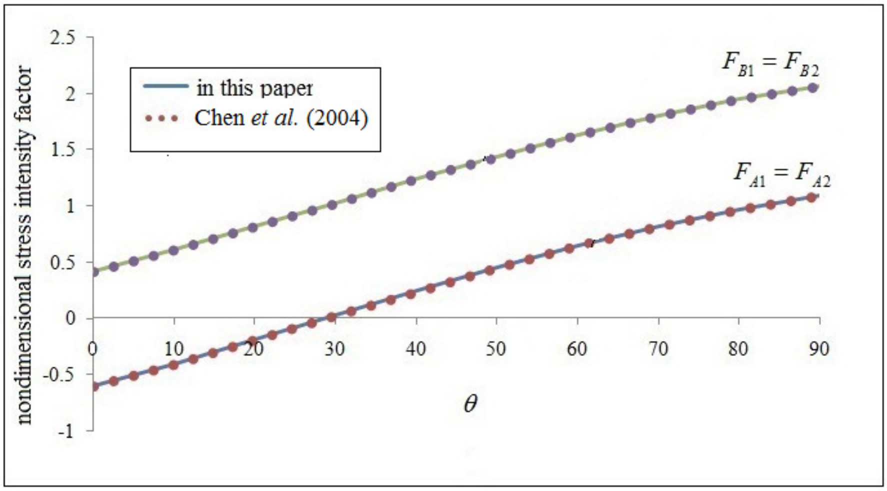

Figure 3: SIFs at cracks tips for $k_1 = 0.5$ and $k_2 = 0.5$

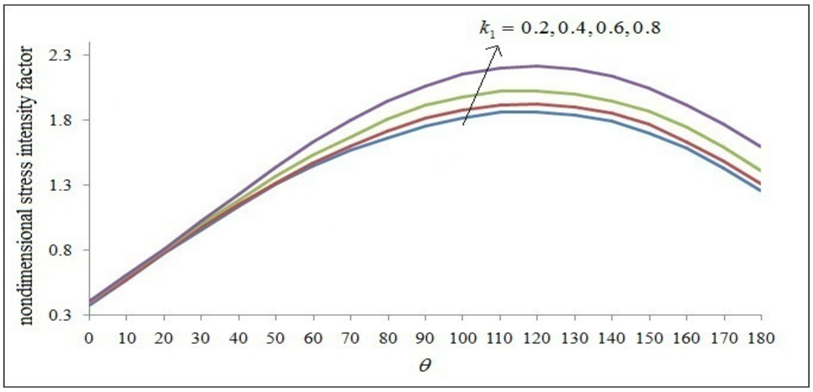

Figure 4 (a): Nondimensionalise SIFs for different values of k_1,
and $k_2 = 0.5$ for F_{B_1} and F_{B_2}

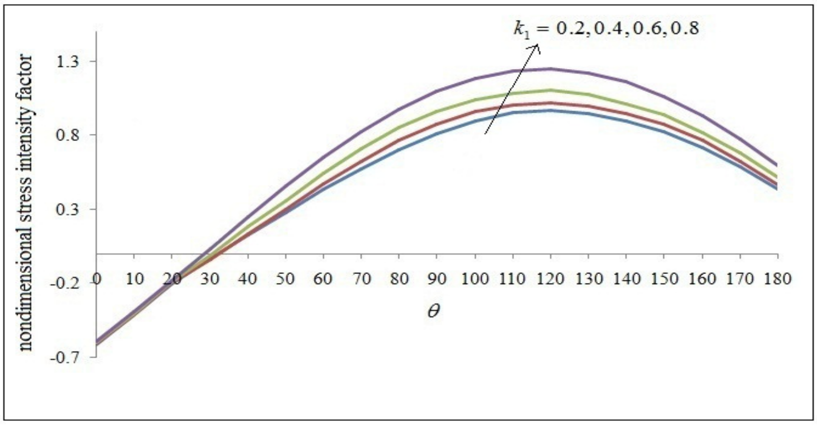

Figure 4 (b): Nondimensionalise SIFs for different values of k_1,
and $k_2 = 0.5$ for F_{A_1} and F_{A_2}

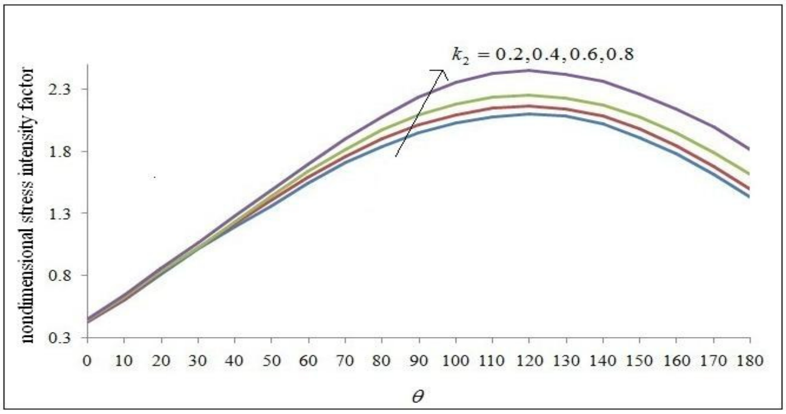

Figure 5 (a): Non dimensionalise SIFs for different values of k_2 , $k_1 = 0.5$ for F_{B_1} and F_{B_2} ,

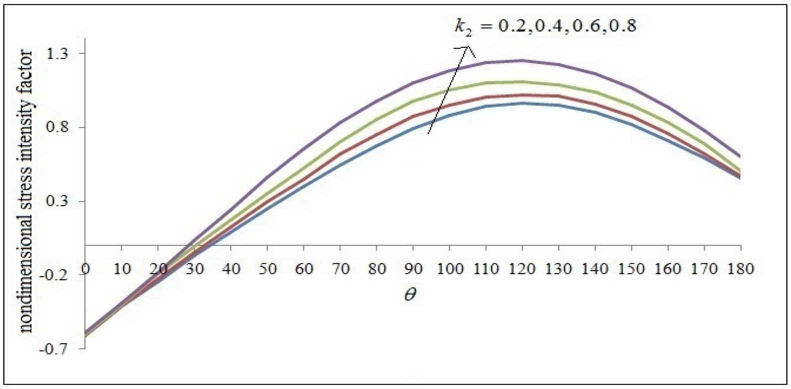

Figure 5 (b): Non dimensionalise SIFs for different values of k_2 , $k_1 = 0.5$ for F_{A_1} and F_{A_2}

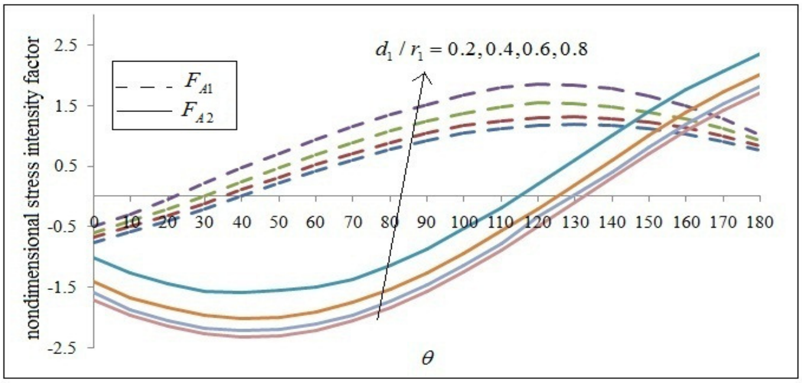

Figure 6 (a): Nondimesionalise SIFs for different values of d_1 / r_1 and $d_2 / r_2 = 0.5$

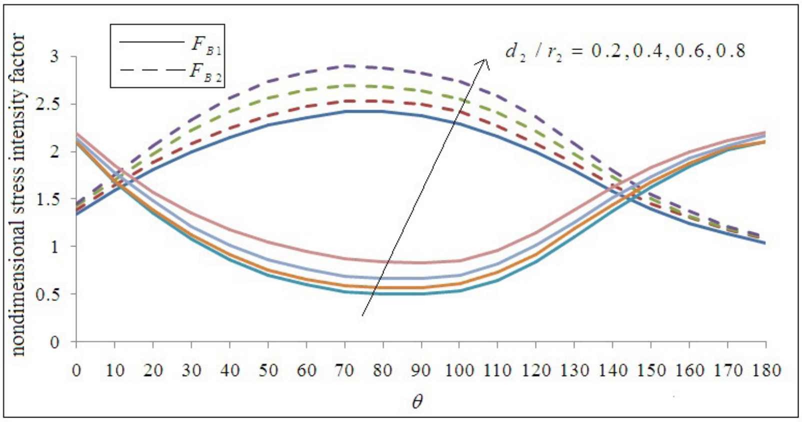

Figure 6 (b): Nondimesionalise SIFs for d_2 / r_2 and $d_1 / r_1 = 0.5$

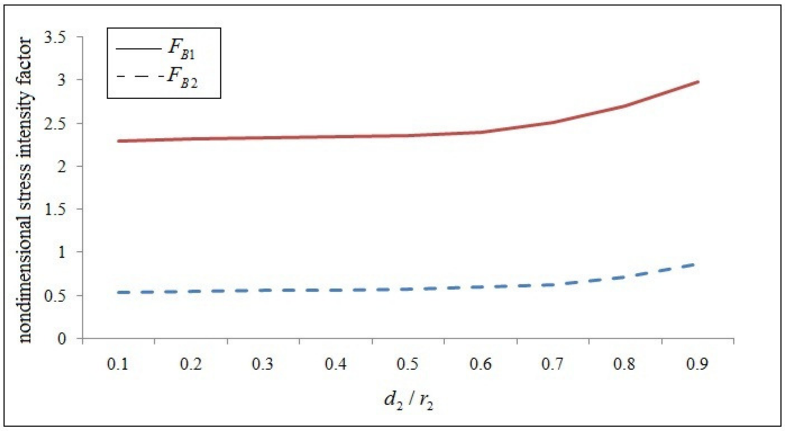

Figure 6 (c): SIFs at $\pi / 2$ when d_2 / r_2 varies and $d_1 / r_1 = 0.5$

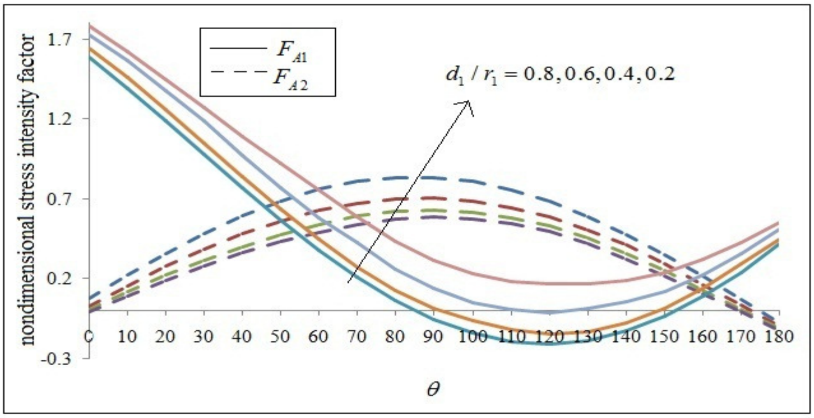

Figure 7 (a): Nondimensionalise SIFs for different values of d_1 / r_1 and $d_2 / r_2 = 0.5$

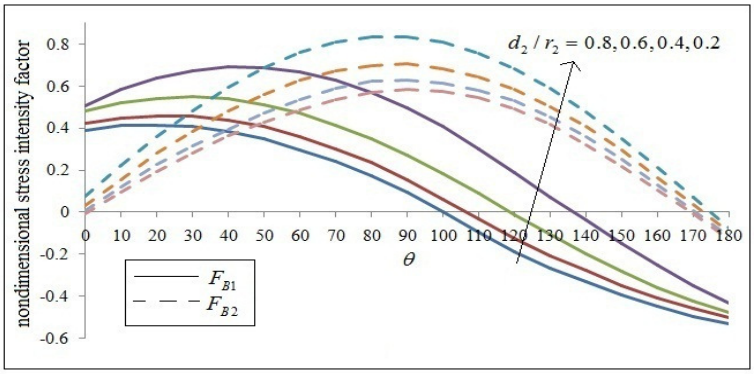

Figure 7 (b): Nondimensionalise SIFs for different values of d_2 / r_2 and $d_1 / r_1 = 0.5$.

5. CONCLUSION

In this paper, the problem of antiplane multiple curved cracks and a circular region is studied. The hypersingular integral equation is formulated by using the complex variable function method. The obtained integral equations are solved numerically. It is found that the SIF increases as the cracks become closer to the circular boundary.

ACKNOWLEDGEMENT

This project is supported by Research University Grant Scheme, Project No:05-03-10-0988RU, Universiti Putra Malaysia.

REFERENCES

Ang, W. T. 2011. A boundary integral approach for plane analysis of electrically semi-permeable planar cracks in a piezoelectric solid. *Eng. Anal. Bound. Elem.* **35**: 647-656.

Chao, C. K. 1996. Interaction between a crack and a circular elastic inclusion under remote uniform heat flow. *Int. J. Solids Struct.* **33**: 3865-3880.

Cheesman, B. A. and Santare, M. H. 2000. The interaction of a curved crack with a circular elastic inclusion. *Int. J. Frac.* **103**: 259-277.

Chen, Y. Z. and Wang, Z. X. 1986. Solutions of multiple crack problems of a circular region with free or fixed boundary condition in antiplane elasticity. *Int. J. Frac*. **30**: 287-293.

Chen, Y. Z. and Hasebe, N. 1992. Interaction of two curved cracks in an innite plate. *Arc. Appl. Mech.* **62**: 147-157.

Chen, Y. Z. 1993. New Fredholm integral equation for multiple crack problem in antiplane elasticity. *Int. J. Frac*. **64**: 63-77.

Chen, W. H. and Chen, T. C. 1995. An efficient dual boundary element technique for a two-fracture problem with multiple cracks. *Int. J. Num. Meth. Eng*. **38**:1739-1756.

Chen, Y. Z. 1999. Stress Intensity factors for curved and kinked cracks in plane extension. *Theo. Appl. Frac. Mech*. **31**: 223-232.

Chen, Y. Z. 2003. A numerical solution technique of hypersingular integral for cracks. *Commun. Num. Meth. Eng*. **19**: 645-655.

Chen, Y. Z., Lin, X. Y. and Wang, Z. X. 2004. Numerical solutions of a hypersingular integral equation for antiplane elastic curved crack problems of circular regions. *Acta Mech*. **173**: 1-11.

Chen, Y. Z. and Lin, X. Y. 2005. Numerical solutions of hypersingular integral equation for curved cracks in circular regions. *Int. J. Frac.* **132**(3): 205-222.

Cotterell, B. and Rice, J. R. 1980. Slightly curved or kinked cracks. *Int. J. Frac*. **16**: 155-169.

Dong, C. Y. 2005. A new integral equation formulation of two-dimensional inclusion crack problems. *Int. J. Solids Struct*. **42**: 5010-5020.

Gray, L. J., Martha, L. F. and Ingraffea, A. R. 1990. Hypersingular integrals in boundary element fracture analysis. *Int. J. Num. Meth. Eng*. **29**: 1135-1158.

Hasebe, N., Keer, L. M. and Nemat-Nasser, S. 1984. Stress analysis of a kinked crack initiation from a rigid line inclusion. *Formulation, Mech. Mat*. **3**: 131-145.

Hong-shan, D., Shao-guang, S. and Lei, Z. 2008. Singular integral equation approach tp III-bifurcated cracks in elastic circular region. *J. Lanzhou Uni. Tech.* **1**: 44.

Jian-Fei, L. and Andrzej, H. 2004. Dynamic interaction between multiple cracks and a circular hole swept by SH waves. *Int. J. Sol. Struct*. **41**: (24-25): 6725-6744.

Lin, W. Z. and Chen, Y. Z. 1989. Multiple cracks inside and outside circular regions. *Theo. Appl. Frac. Mech.* **11**: 199-208.

Martin, P. A. 2000. Pertubated cracks in two dimension: an integral-equation approach. *Int. J. Frac*. **104**: 317-327.

Mayrofer, K. and Fischer, F. D. 1992. Derivation of a new analytical solution for a general two dimensional Finite-part integral applicable in fracture mechanics. *Int. J. Num. Meth. Eng*. **33**: 1027-1047.

Muskhelishvili, N. I. and Radok, J. R. M. 1957. *Some basic problems of the mathematical theory of elasticity*. Leyden: Noordho Int. Pub.

Nik Long, N. M. A. and Eshkuvatov, Z. K. 2009. Hypersingular Integral Equation for multiple curved crack problem in plane elasticity. *Int. J. Solids Sruct*. **46**: 2611-2617.

Shen, L. J. and Weiping, Y. H. 1998. A study of crack problem in a circular region of a solid with antiplane multiple holes. *Chinese Quart. Mech*. **4**: 10.

Yan, X. 2010. A boundary element analysis for stress intensity factors of multiple circular arc cracks in a plane elasticity plate. *Appl. Math. Mod.* **34**: 2722-2737.

Zhong-xian, W. and Lei, Z. 2006. Singular integral equation approach for edge crack problems of circular region in antiplane elasticity. *J. Jiangsu Uni*. **3**: 21.